Replication protein A dynamically regulates monoubiquitination of proliferating cell nuclear antigen

Received for publication, August 10, 2018, and in revised form, January 17, 2019 Published, Papers in Press, January 30, 2019, DOI 10.1074/jbc.RA118.005297

Mark Hedglin[1], **Mahesh Aitha**, **Anthony Pedley**, **and Stephen J. Benkovic**

From the Department of Chemistry, The Pennsylvania State University, University Park, Pennsylvania 16802

Edited by Patrick Sung

DNA damage tolerance permits bypass of DNA lesions encountered during S-phase and may be carried out by translesion DNA synthesis (TLS). Human TLS requires selective monoubiquitination of proliferating cell nuclear antigen (PCNA) sliding clamps encircling damaged DNA. This post-translational modification (PTM) is catalyzed by Rad6/Rad18. Recent studies revealed that replication protein A (RPA), the major ssDNA-binding protein, is involved in the regulation of PCNA monoubiquitination and interacts directly with Rad18 on chromatin and in the nucleoplasm. However, it is unclear how RPA regulates this critical PTM and what functional role(s) these interactions serve. Here, we developed an *in vitro* assay to quantitatively monitor PCNA monoubiquitination under *in vivo* scenarios. Results from extensive experiments revealed that RPA regulates Rad6/Rad18 activity in an ssDNA-dependent manner. We found that "DNA-free" RPA inhibits monoubiquitination of free PCNA by directly interacting with Rad18. This interaction is promoted under native conditions when there is an overabundance of free RPA in the nucleoplasm where Rad6/Rad18 and a significant fraction of PCNA reside. During DNA replication stress, RPA binds the ssDNA exposed downstream of stalled primer/template (P/T) junctions, releasing Rad6/Rad18. RPA restricted the resident PCNAs to the upstream duplex regions by physically blocking diffusion of PCNA along ssDNA, and this activity was required for efficient monoubiquitination of PCNA on DNA. Furthermore, upon binding ssDNA, RPA underwent a conformational change that increased its affinity for Rad18. Rad6/Rad18 complexed with ssDNA-bound RPA was active, and this interaction may selectively promote monoubiquitination of PCNA on long RPA-coated ssDNA.

In eukaryotes, the replicative DNA polymerases (pols)[2] anchor to PCNA sliding clamps encircling DNA to achieve the high degree of processivity required for efficient DNA replication (1). Under native conditions, the replicative pols are rate-limited by unwinding of double-stranded DNA (dsDNA) such that template bases are replicated as soon as they are available. This tight coupling limits exposure of ssDNA. However, the stringent replicative pols cannot accommodate distortions to the native DNA sequence. Prominent examples of these are modifications (lesions) to the native template bases from exposure to reactive metabolites and environmental mutagens such as UV radiation. Consequently, DNA synthesis on the afflicted template abruptly stops upon encountering these lesions but unwinding of dsDNA continues. These "uncoupling" events expose long stretches of the damaged template that are immediately coated by RPA, a heterotrimeric complex comprised of RPA70, RPA32, and RPA14 subunits. RPA is the major eukaryotic ssDNA-binding complex and protects exposed ssDNA from degradation and prevents formation of alternative DNA structures that are refractory to DNA synthesis (2). dsDNA unwinding eventually stalls after an uncoupling event and failure to re-couple DNA synthesis and dsDNA unwinding often results in dsDNA breaks that may lead to gross chromosomal rearrangements, cell-cycle arrest, and cell death. These replicative arrests may be overcome by TLS where specialized TLS pols bind to the resident PCNA and replicate the damaged DNA, allowing DNA synthesis by a replicative pol to resume (2). In humans, TLS requires monoubiquitination of PCNA encircling stalled P/T junctions and this critical PTM is catalyzed by Rad6/Rad18 (3, 4).

Rad6 is an E2 ubiquitin-conjugating enzyme that catalyzes covalent attachment of ubiquitin to a lysine residue within a target protein. On its own, Rad6 does not bind PCNA and is incapable of modifying PCNA. Furthermore, Rad6 alone can monoubiquitinate other Rad6 molecules and form mixed ubiquitin chains. The latter requires the noncovalent ubiquitin-binding site on Rad6. Selection of a target protein for Rad6 is dictated by an E3 ubiquitin ligase, such as Rad18, that simultaneously binds Rad6 and a target protein. Rad18 only functions as a homodimer and dimerization occurs through an N-terminal RING domain (Fig. S1). A Rad18 homodimer interacts with a Rad6 through two independent binding sites (4). A distinct region of a Rad18 RING domain recognizes Rad6 through a canonical interface that is conserved among all E2/E3 RING complexes (5, 6). Also, the C-terminal Rad6-binding (R6B) domain of a Rad18 binds the noncovalent ubiquitin-binding site of Rad6, preventing mixed ubiquitin chain formation (7). In addition to the RING domain, the N-terminal half of Rad18

This work was supported by National Institute of General Medical Sciences (NIGMS), National Institutes of Health Grant R01 GM013306. The authors declare that they have no conflicts of interest with the contents of this article. The content is solely the responsibility of the authors and does not necessarily represent the official views of the National Institutes of Health.

This article contains Figs. S1–S10, Table S1, and supporting information.

[1] To whom correspondence should be addressed: Tel.: 814-863-1080; E-mail: muh218@psu.edu.

[2] The abbreviations used are: pols, polymerases; PCNA, proliferating cell nuclear antigen; RPA, replication protein A; P/T, primer/template; R6B, Rad6-binding; poly(dT)$_{33}$, 33-mer poly(dT); OB, oligonucleotide-binding; WH, winged helix; RFC, replication factor C; PTM, posttranslational modification; TCEP, tris(2-carboxyethyl)phosphine; KOAc, potassium acetate; SSB, single-strand DNA–binding protein.

contains multiple independent binding domains, one of which directly interacts with PCNA. Thus, Rad18 activates and targets Rad6 toward PCNA and only permits monoubiquitination (4).

Recent cellular studies revealed that RPA is involved in the regulation of PCNA monoubiquitination by Rad6/Rad18 and interacts with Rad18 on chromatin and in the nucleoplasm (*i.e.* nonchromatin associated/soluble fraction). Interestingly, the latter are quite prominent in nonperturbed human cells (8–10). However, it is unclear how RPA regulates this critical PTM and what functional role(s) these interactions serve. To address this, we developed an *in vitro* fluorescent assay to quantitatively monitor the effect of RPA on PCNA monoubiquitination under conditions that mimic *in vivo* scenarios.

Results

Rad6/Rad18 monoubiquitinates free PCNA

Rad6/Rad18 is active throughout the cell cycle and does not require PCNA to encircle DNA for monoubiquitination of PCNA to occur (4, 6, 7, 11–18). Interestingly, PCNA protein levels are overabundant and essentially maintained throughout the cell cycle such that at least 30% of the PCNA pool resides in the nucleoplasm (*i.e.* free in solution) at any time. Particularly, free PCNA accounts for more than 80% of the pool throughout G_1 and G_2/M, which collectively last ~16 h in rapidly proliferating human cells (19–23). Accordingly, we initially focused on monoubiquitination of free PCNA in solution over a biologically relevant time scale that approaches G_1 phase (~11 h) of rapidly proliferating human cells (19). To comprehensively and quantitatively study PCNA monoubiquitination, we utilized fluorescence to monitor the attachment of ubiquitin to all proteins present. Human ubiquitin is devoid of cysteine and residue Glu-24 (Fig. S2*A*) is far removed from both the "hydrophobic patch" where ubiquitin-binding domains dock and the C-terminal glycine residue where target proteins are attached (24). Residue Glu-24 was mutated to cysteine (E24C) and labeled with fluorescein (Fig. S2*B*). All lysine residues of ubiquitin remain available for conjugation into polyubiquitin chains (7).

The attachment of ubiquitin to proteins requires Rad6/Rad18 (Fig. 1*A*, compare *lanes 1–5* to *lanes 8* and *9*) and increases over time such that 2690 nM ± 61.7 nM ubiquitin is conjugated to proteins at 8 h (Fig. 1*B*). At this concentration, ~90% of the total ubiquitin is conjugated to proteins and the fluorescence signal remains constant (Fig. S2*C*). Thus, attachment of fluorescein-labeled ubiquitin to proteins does not affect the fluorescence output of the dye, permitting quantitative analysis. The ubiquitinated proteins range in size from ~20–150 kDa (Fig. 1*A*). In human cells, Rad18 is monoubiquitinated by Rad6 at four conserved lysine residues (Fig. S1) (25). This process has previously been reconstituted *in vitro* with recombinant human proteins and is indicated by the appearance of bands greater than 75 kDa in size (6, 7). As expected, these bands are only observed in the presence of Rad6/Rad18 (Fig. 1*A*, compare *lanes 1–5* to *lanes 8* and *9*) but are independent of PCNA (Fig. 1*A*, compare *lanes 1–5* to *lanes 6* and *7*; Fig. S3*A*, compare *lanes 1* and *2* to *lanes 3* and *4*). Western blotting confirmed the identity of these bands as ubiquitinated Rad18 (Fig. S3*A*, *lanes 13–16*). Rad18 is clearly the predominant ubiquitinated species and increases in fluorescence intensity over time (Fig. 1*A*, *lanes 1–5*). 2610 ± 63.6 nM of ubiquitin is conjugated to Rad18 over the incubation (Fig. 1*B*), indicating that each Rad18 contains approximately two ubiquitin moieties on average.

A distinct band appears between 20–25 kDa in size and increases in fluorescence intensity over time (Fig. 1*A*, *lanes 1–5*). This band is only observed in the presence of Rad6/Rad18 (Fig. 1*A*, compare *lanes 1–5* to *lanes 8* and *9*) and is independent of PCNA (Fig. 1*A*, compare *lanes 1–5* to *lanes 6* and *7*; Fig. S3*A*, compare *lanes 1* and *2* to *lanes 3* and *4*). The molecular weight of Rad6 increases from ~15 kDa to ~24 kDa by the attachment of ubiquitin and Rad6 will monoubiquitinate itself in the absence of functional interactions with Rad18 (7). Western blotting confirmed the identity of this band as monoubiquitinated Rad6 (Fig. S3*A*, *lanes 9–12*). Only 17.7 ± 1.62 nM of ubiquitin is conjugated to Rad6 at 8 h (Fig. 1*B*). Thus, monoubiquitinated Rad6 is minimal, accounting for less than 3% of the total Rad6 present.

In the presence of PCNA and Rad6/Rad18 (Fig. 1*A*, *lanes 1–5*), a distinct band appears between 40 and 50 kDa and increases in intensity over time. This band disappears when PCNA is removed (Fig. 1*A*, compare *lanes 1–5* to *lanes 6* and *7*; Fig. S3*A*, compare *lanes 1* and *2* to *lanes 3* and *4*). The molecular weight of a PCNA monomer increases from ~36 kDa to ~45 kDa by the attachment of ubiquitin (Fig. S3*C*) and Rad6/Rad18 will monoubiquitinate PCNA in solution (6, 7, 17, 18). Western blotting confirmed the identity of this band as monoubiquitinated PCNA (Fig. S3*A*, *lanes 5–8*). 71.1 ± 6.79 nM ubiquitin is conjugated to PCNA monomers over the incubation (Fig. 1*B*). At this concentration, 23.6 ± 2.25% of PCNA monomers are monoubiquitinated (Fig. 1*C*), which equates to 70.7 ± 6.76% of all PCNA homotrimers containing a single ubiquitin, on average. Altogether, these results indicate that 1) ubiquitinated Rad18 (which accounts for all Rad18 present) binds to and is functional with Rad6, 2) Rad6 and Rad18 maintain active/productive interactions throughout the incubation, and 3) Rad6/Rad18 monoubiquitinates free PCNA and this activity is prominent over a biologically relevant time scale.

RPA regulates monoubiquitination of free PCNA in a ssDNA-dependent manner

Rad6/Rad18 complexes are prominent in nonperturbed human cells and predominantly observed in the soluble fraction (*i.e.* nonchromatin associated) (8–10). Next, we repeated the assays described in Fig. 1 in the presence of free RPA. At the highest RPA concentration (6 μM), additional ubiquitinated species do not appear in fluorescence scans (Figs. S4 and S5) and ubiquitination of RPA subunits is not observed by Western blotting (Fig. S5). Thus, Rad6/Rad18 does not conjugate ubiquitin to free RPA and, hence, any observed effects are not attributable to RPA ubiquitination. Monoubiquitination of proteins (total) is slightly reduced over the range of RPA concentrations (Fig. 2) and this is primarily because of the minor reduction in Rad18 monoubiquitination. However, RPA dramatically stimulates monoubiquitination of Rad6 and such behavior is independent of PCNA (Fig. S4). Monoubiquitination of free PCNA is significantly reduced over the range of RPA concentrations,

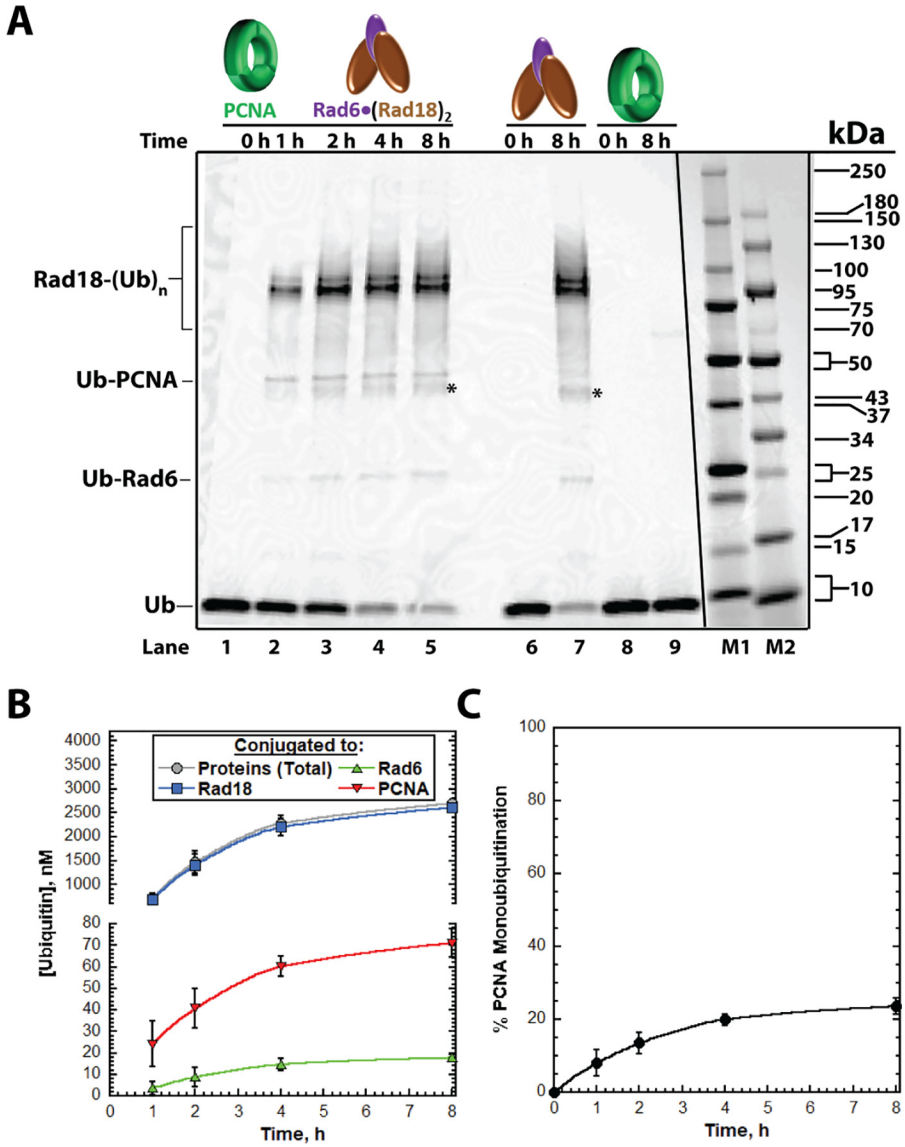

Figure 1. Ubiquitination of target proteins. *A*, fluorescence scan. Molecular mass (in kDa) of markers (*lanes M1* and *M2*) are indicated. Ubiquitin (*Ub*), monoubiquitinated PCNA (*Ub-PCNA*), monoubiquitinated Rad18 (*Rad18-(Ub)$_n$*), and monoubiquitinated Rad6 (*Ub-Rad6*) are indicated. The identities of Ub-PCNA, Rad18-(Ub)$_n$, and Ub-Rad6 were confirmed by Western blotting (Fig. S3*A*). Asterisk indicates ubiquitination of a common, minor truncation product of recombinant human Rad18 (Fig. S3*B*). *B* and *C*, quantitative analysis of monoubiquitination. Data represent the average ± S.D. of three independent experiments. *B*, monoubiquitination of proteins. The concentrations of ubiquitin conjugated to proteins (total), Rad18, Rad6, and PCNA are plotted as a function of time. Symbols for each are indicated in the figure legend. *C*, extent of PCNA monoubiquitination. The percentage of PCNA monomers that are monoubiquitinated is plotted as a function of time.

and identical results are observed by Western blotting (Fig. S4). Thus, RPA directly inhibits monoubiquitination of free PCNA by Rad6/Rad18. It should be noted that RPA was limited to ≤6 μM to maintain physiological ionic strength. At this concentration, RPA is only present at a 5-fold excess over Rad18. RPA is the most abundant ssDNA-binding protein in human cells and this high concentration is maintained throughout the cell cycle such that RPA is at least 100-fold in excess of Rad18 in unperturbed human cells (26, 27). RPA:Rad18 ratios that approach physiological conditions are likely to further inhibit monoubiquitination of free PCNA.

Rad6/Rad18 activity is imperative during DNA damage tolerance when RPA coats persistent ssDNA regions exposed by uncoupling events at replication-blocking lesions (2). Hence, the observed inhibition of Rad6/Rad18 activity by free RPA must be relieved in the presence of ssDNA. To test this, we monitored the effect of ssDNA on the RPA-dependent inhibition of free PCNA monoubiquitination. We repeated the assays described above except RPA was first pre-incubated with a 33-mer poly(dT) ssDNA template (poly(dT)$_{33}$) (Fig. S6). At physiological ionic strength, human RPA binds ssDNA with extremely high affinity (K_D ~ fM to pM), low cooperativity, and an occluded binding site size of 30 ± 2 nt (28, 29). Furthermore, nearly all ssDNA (24 ± 1 nt) occluded by a single RPA directly interacts with the protein (28–30). In contrast, human Rad18 has relatively weak affinity (K_D ~ nM to μM) for purely ssDNA at minimal ionic strength (~5 mM) and requires at least 49 nucleotides for binding to be observed (17). Thus, occupation of the poly(dT)$_{33}$ ssDNA by Rad6/Rad18 will be minimal, if at all. Indeed, binding of RPA to poly(dT)$_{33}$ is stoichiometric at phys-

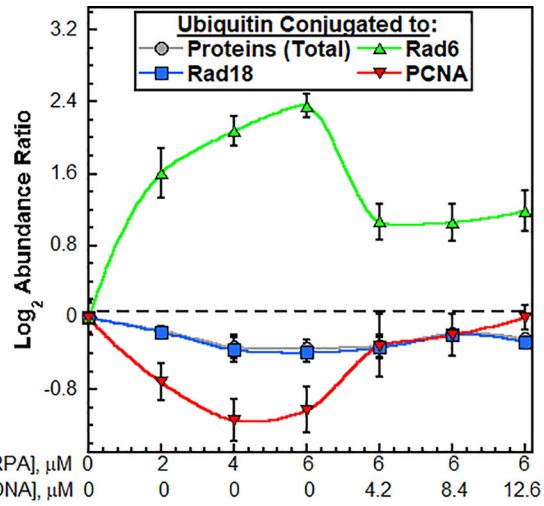

Figure 2. RPA regulates monoubiquitination of free PCNA in a ssDNA-dependent manner. For each concentration of RPA, the amount of ubiquitin attached to a given protein at 8 h incubation is directly compared with that obtained in the absence of RPA (Fig. 1), yielding an abundance ratio. The $\log_2$ of the abundance ratios is plotted as a function of RPA concentration. *Dashed line* indicates no change (0.0). Symbols are indicated in the figure legend and data represent the average ± S.D. of three independent experiments. Assays were carried out with RPA alone or with RPA pre-incubated with poly(dT)$_{33}$ ssDNA (0–12.6 μM).

iological ionic strength whereas binding of Rad6/Rad18 does not occur (Fig. S7 and Table S1). In the presence of excess ssDNA, additional ubiquitinated species do not appear in fluorescence scans (Figs. S5 and S8) and ubiquitination of RPA subunits is not observed by Western blotting (Fig. S5). Together with that described above, this indicates that RPA is not a ubiquitination target of Rad6/Rad18, confirming a recent report (31). Thus, any observed effects in the presence of ssDNA are not attributable to new ubiquitination events.

The minor reductions in monoubiquitination of proteins (total) and Rad18 are essentially maintained over the range of ssDNA concentrations (Fig. 2). Hence, the observed effects on overall protein monoubiquitination are intimately correlated with Rad18 monoubiquitination. However, the RPA-dependent stimulation of Rad6 monoubiquitination is significantly diminished whereas monoubiquitination of free PCNA is restored to the levels observed in the absence of RPA but not beyond. Similar behavior is observed for PCNA by Western blotting (Fig. S8), indicating that RPA/ssDNA complexes do not activate Rad6/Rad18 catalysis. Altogether, this indicates that binding of ssDNA by RPA directly reverses RPA-dependent inhibition of free PCNA monoubiquitination by Rad6/Rad18. Furthermore, it is clear that the effects of RPA and ssDNA on monoubiquitination of Rad6 and free PCNA are inversely correlated.

RPA·Rad18 interactions are direct and enhanced by ssDNA

Four oligonucleotide-binding (OB) folds mediate binding of an RPA to ssDNA. OB-A and OB-B within the RPA70 subunit are the primary ssDNA-binding sites and together comprise an occluded ssDNA-binding site of 8 nt. Interestingly, these OB folds also comprise one of the two independent Rad18-binding sites (8, 27, 32). OB-C and OB-D reside in the RPA70 and RPA32 subunits, respectively, and extend the occluded ssDNA-binding site to 30 ± 2 nt (27–29, 32). The RPA32 subunit also contains a winged helix (WH) domain that is largely responsible for the interaction of RPA with cellular proteins, and the accessibility of this domain is enhanced upon ssDNA binding (33, 34). The second independent Rad18-binding site within RPA resides in RPA32 but has yet to be mapped (8, 10). The results from Fig. 2 indicate that RPA directly mediates Rad6/Rad18 activity toward free PCNA in a ssDNA-dependent manner. To gain insight into how this occurs we analyzed the interaction of RPA and Rad6/Rad18 as well as the composition of Rad6/Rad18 by analytical gel filtration.

Rad6/Rad18 alone peaks at 21.6 min retention time (Fig. 3*A*), and the appearance and disappearance of Rad18 and Rad6 are intimately correlated, indicating a stable binding interaction between these proteins. RPA alone peaks at 25.1 min retention time (Fig. 3*B*). When RPA and Rad6/Rad18 are pre-incubated, the Rad6/Rad18 peak undergoes a small shift to a higher molecular weight and a small increase in intensity (Fig. 3*C*, *top panel*). Furthermore, the RPA70 and RPA32 subunits elute in earlier fractions (Fig. 3*C*, *bottom panel*). Together, this indicates that RPA interacts directly, albeit weakly, with Rad18 at physiological ionic strength in the absence of any nucleic acid, in agreement with previous *in vivo* and *in vitro* studies (8). In the absence of ssDNA, both Rad18-binding sites within RPA are potentially available and, hence, it cannot be deciphered if one or both contribute to the observed interaction.

The tight correlation of the Rad18 and Rad6 elution profiles (Fig. 3*A*, *bottom panel*) is unaffected by RPA (Fig. 3*C*, *bottom panel*), and RPA does not decrease the amount of Rad6 that co-elutes with Rad18 (Fig. 3*F*), indicating that RPA does not preclude Rad18 from binding Rad6. Furthermore, mixed ubiquitin chain formation by Rad6 is not observed under any experimental condition described above. This activity requires noncovalent binding of ubiquitin to Rad6 and is prohibited by the Rad18 R6B, which effectively outcompetes ubiquitin for binding to Rad6 (Fig. S9) (7). Collectively, these results indicate that the R6B domain of Rad18 remains bound to the noncovalent ubiquitin-binding site of Rad6 throughout all incubations. Next, we repeated these assays in the presence of ssDNA.

Binding of Rad6/Rad18 to ssDNA does not occur when the concentrations of poly(dT)$_{33}$ and RPA are stoichiometric (Fig. S7 and Table S1). Rather, all RPA and ssDNA reside in a complex (Fig. 3*D*, *top panel*; Fig. S7; and Table S1) in which RPA occupies the entire length of the ssDNA (28, 29). Thus, any retention of Rad6/Rad18 by the RPA/ssDNA complex is through a direct interaction between RPA and Rad18. The Rad6/Rad18 peak (Fig. 3*A*, *top panel*) undergoes a small shift to a higher molecular weight and a significant increase in intensity (Fig. 3*E*, *top panel*). Furthermore, greater amounts of Rad18 are observed in the early fractions with RPA and ssDNA (Fig. 3*E*, *bottom panel*) compared with RPA alone (Fig. 3*C*, *bottom panel*). Finally, greater amounts of the RPA70 and RPA32 subunits are observed in the early fractions with Rad6/Rad18 and ssDNA (Fig. 3*E*, *bottom panel*) compared with Rad6/Rad18 alone (Fig. 3*C*, *bottom panel*) or ssDNA alone (Fig. 3*D*, *bottom panel*). This indicates that ssDNA-bound RPA directly interacts with Rad6/Rad18 at physiological ionic strength and ssDNA enhances the affinity of RPA for Rad6/Rad18, confirm-

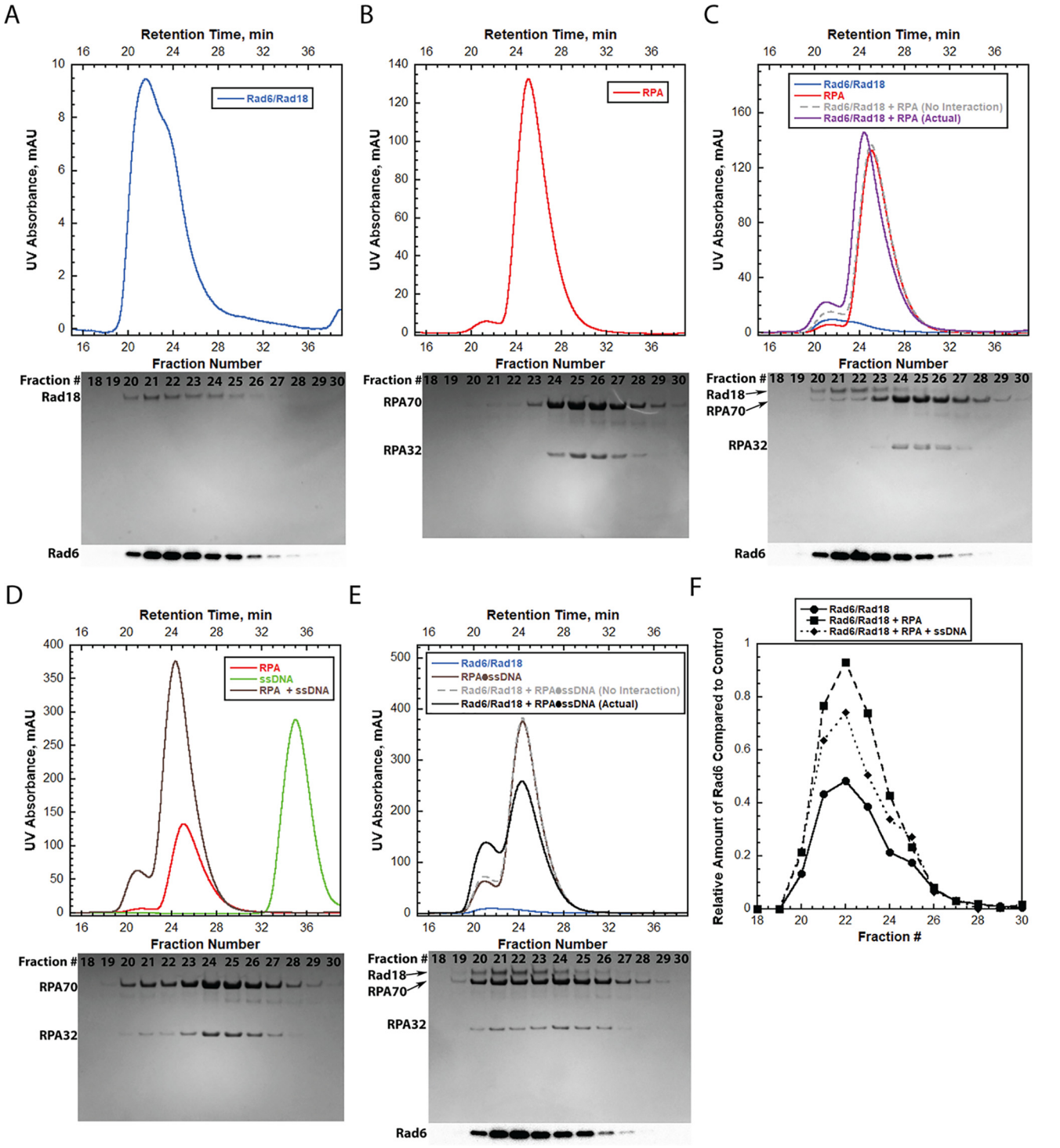

Figure 3. The Rad18·RPA is direct and enhanced by ssDNA. *A–E*, analytical gel filtration analyses of the interaction of RPA with Rad6/Rad18. Chromatograms of Rad6/Rad18 (9.27 μM), RPA (46.6 μM), RPA·ssDNA (46.6 μM RPA + 46.4 μM poly(dT)$_{33}$), or pre-incubated complexes thereof are shown in the *top panels*. The predicted elution profile for no interaction (*dashed gray line*) were determined by adding the elution profiles of the individual components. SDS-PAGE analyses of fractions 18–30 from the analytical gel filtration columns are shown in the *bottom panels*. Rad18 and RPA subunits (RPA70, RPA32) were visualized by Coomassie Blue staining and indicated. Rad6 was visualized by Western blotting and indicated. *F*, Rad6 elution. The amount of Rad6 that elutes in each fraction was quantified, normalized to a loading control, and plotted.

ing previous hypotheses (8–10). The tight correlation of the Rad18 and Rad6 elution profiles (Fig. 3, *A* and *C*, *bottom panels*) remains unaffected by ssDNA (Fig. 3*E*, *bottom panel*) and ssDNA does not decrease the amount of Rad6 that co-elutes with Rad18 (Fig. 3*F*). Thus, RPA (in the absence or presence of ssDNA) does not preclude Rad18 from binding Rad6.

Prohibiting diffusion of PCNA along ssDNA is required for efficient PCNA monoubiquitination at P/T junctions

Previous studies revealed that RPA is required for monoubiquitination of PCNA at ssDNA regions generated by uncoupling events during S-phase (8, 9). Similarly, Rad6/Rad18-catalyzed monoubiquitination of PCNA occurs outside of S-phase

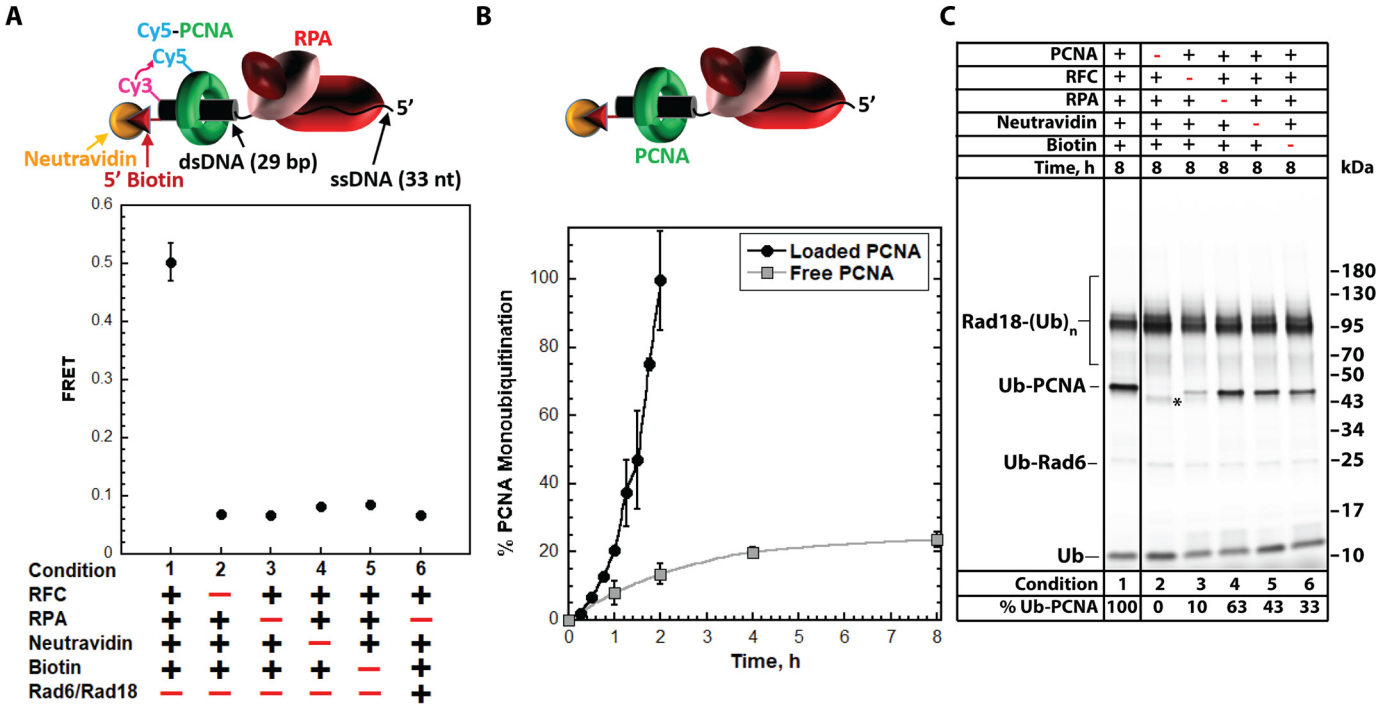

Figure 4. RPA promotes monoubiquitination of PCNA encircling P/T DNA by prohibiting diffusion of PCNA along ssDNA. *A*, monitoring the retention of PCNA on DNA through FRET. *Top*, schematic representation of FRET experiments. Cy5-PCNA was assembled on the Cy3P/BioT33 DNA substrate in the presence of RPA, and FRET was monitored at equilibrium. When loaded onto the Cy3P/BioT33 DNA substrate, the Cy5 FRET acceptor on PCNA faces the Cy3 FRET donor on the P/T DNA. At equilibrium, Cy5-PCNA can be excited through FRET from Cy3P/BioT33 only when the two dyes are held in close proximity (< ~10 nm). *Bottom*, characterization of steady-state FRET. Cy5-PCNA was assembled onto the Cy3P/BioT33 DNA substrate with various components omitted and FRET was measured. *B*, monoubiquitination of PCNA encircling DNA. PCNA was pre-assembled onto the P/BioT33 DNA substrate (Fig. S6) and then monoubiquitination of target proteins was monitored as described in Figs. 1 and 2. *Top*, schematic representation of PCNA assembled onto the P/BioT33 DNA substrate (*i.e. Loaded PCNA*). *Bottom*, extent of PCNA monoubiquitination. The percentage of PCNA monomers that are monoubiquitinated is plotted as a function time. Data represent the average ± S.D. of three independent experiments. Data (*Loaded PCNA*) are overlaid on data from Fig. 1*C* (*Free PCNA*) for comparison. *C*, fluorescence scan of ubiquitination reactions lacking a single reaction component. Experimental conditions (1–6) are indicated below each lane. Samples for all conditions are from the same gel. A lane splice is indicated by a *vertical black line*. *Condition 1* serves as a control in which all reaction components are included. Bands are indicated as in Figs. 1 and 2. The percentage of PCNA monomers that are monoubiquitinated at 8 h incubation (*% Ub-PCNA*) is indicated below each lane.

at DNA repair sites and this activity prevents formation of dsDNA breaks and requires RPA (13, 16). However, it is unknown how RPA promotes monoubiquitination of PCNA encircling P/T junctions. We recently discovered that RPA bound to the exposed ssDNA adjacent to a P/T junction restricts PCNA to the upstream duplex region by physically blocking diffusion of PCNA along ssDNA (35). Thus, RPA may promote monoubiquitination of PCNA on DNA by stabilizing PCNA at/near stalled P/T junctions. To test this, we thoroughly characterized monoubiquitination of PCNA encircling a P/T DNA substrate (P/BioT33) (Fig. S6).

The biotin label at the duplex end is pre-bound with NeutrAvidin. The ssDNA region (33 nt) accommodates a single RPA molecule at physiological ionic strength and is pre-bound with stoichiometric RPA. Together, RPA and the biotin/NeutrAvidin complex stabilize loaded PCNA on the DNA substrate by serving as physical blocks to PCNA diffusion (35). PCNA is pre-loaded onto the DNA substrate by the clamp loader, replication factor C (RFC). The RPA/DNA complex is present in slight excess (10%) of PCNA to eliminate free PCNA in solution. Thus, all PCNA is loaded onto DNA and stabilized (Fig. 4*A*, *Condition 1*) (36). Under these conditions, monoubiquitination of PCNA is significantly enhanced (Fig. 4*B*) such that 20.48% ± 0.4160% of PCNA monomers are monoubiquitinated in 1 h and all PCNA monomers are monoubiquitinated in ≤2 h. Western blotting confirmed complete monoubiquitination of PCNA (Fig. S10). In contrast, monoubiquitination of ~20% of PCNA monomers requires at least 8 h when PCNA is free in solution, indicating that stabilization of loaded PCNA on P/T DNA enhances monoubiquitination of PCNA by Rad6/Rad18 at least 8-fold. To gain further insight, we repeated these assays by selectively omitting individual components (Fig. 4*C*).

When RFC is omitted, PCNA is not assembled onto the DNA substrate (Fig. 4*A*, *Condition 2*) and only 10% of PCNA monomers are monoubiquitinated at 8 h incubation (Fig. 4*C*, *Condition 3*). This level of PCNA monoubiquitination is observed in 30–45 min when RFC is included (Fig. 4*B*), suggesting that loading of PCNA onto P/T DNA by RFC significantly enhances monoubiquitination of PCNA by Rad6/Rad18. In the absence of either NeutrAvidin or biotin, PCNA is loaded onto the DNA substrate but immediately diffuses off the duplex end upon release from RFC (Fig. 4*A*, *Conditions 4* and *5*) (35). Under these conditions, only 33–43% of PCNA monomers are monoubiquitinated at 8 h incubation (Fig. 4*C*, *Conditions 5* and *6*). This level of PCNA monoubiquitination is observed in ~1.25 h when the NeutrAvidin/biotin block is intact (Fig. 4*B*). Thus, loading and stabilization of PCNA on P/T DNA are both required for the observed enhancement of PCNA monoubiquitination on DNA (Fig. 4, *B* and *C*). When RPA is omitted, PCNA is loaded onto the DNA substrate but immediately dif-

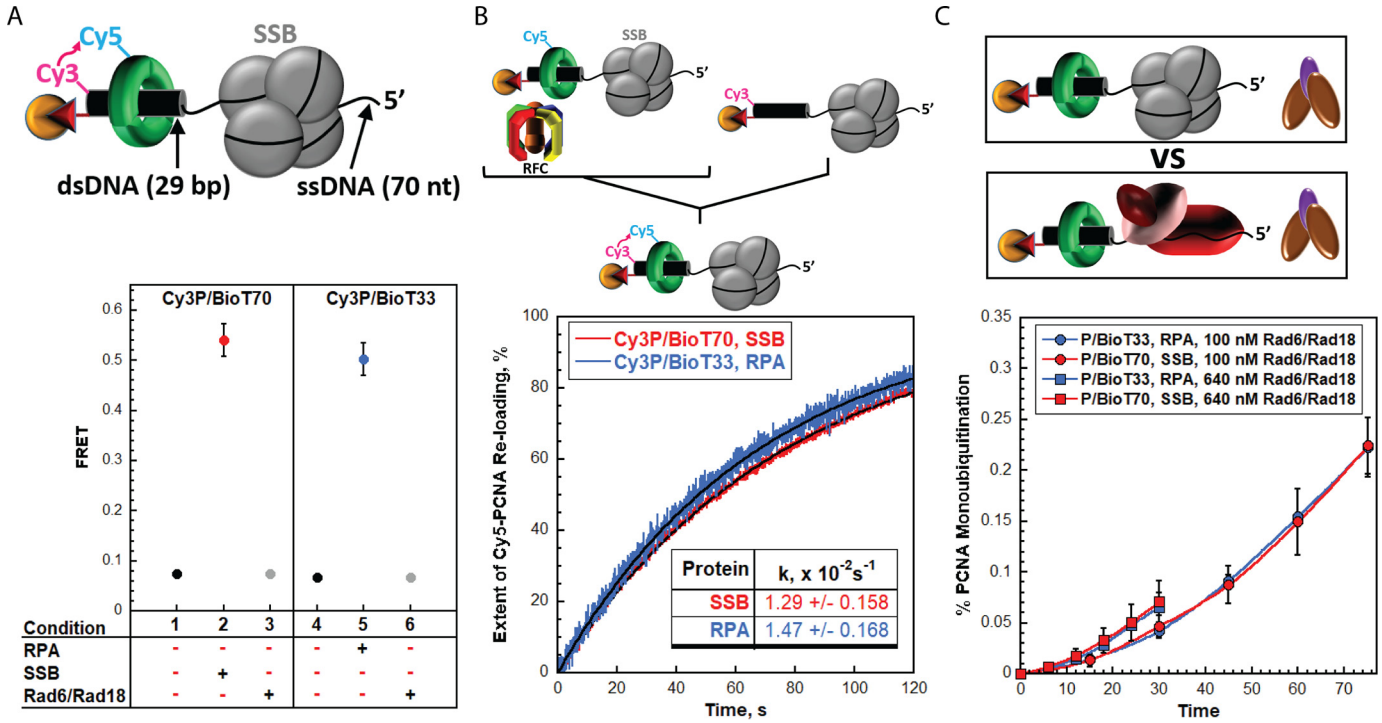

Figure 5. The stability of PCNA encircling a stalled P/T junction drives PCNA monoubiquitination. *A*, retention and orientation of PCNA on DNA. *Top*, schematic representation of the FRET experiments. Cy5-PCNA was assembled on the Cy3P/BioT70 DNA substrate (Fig. S6) in the presence of SSB, and FRET was monitored at equilibrium as in Fig. 4*A*. *Bottom*, FRET in the presence of SSB. FRET is only observed for the Cy3P/BioT70 DNA substrate when SSB is included (*Condition 2*); excess Rad6/Rad18 will not compensate (*Condition 3*). Identical results are observed for RPA with the Cy3P/BioT33 DNA substrate (*Conditions 4–6*). As observed in a previous report, the FRET measured in the presence of SSB (*Condition 2*, 0.540 ± 0.0327) and RPA (*Condition 5*, 0.502 ± 0.0327) are within experimental error, indicating that the same amount of PCNA is loaded onto and stabilized at a P/T junction in the same FRET state (*i.e.* orientation) when the adjacent ssDNA is bound by either RPA or SSB. *B*, stability of PCNA encircling DNA. *Top*, schematic representation of the experiment. Cy5-PCNA is pre-assembled onto unlabeled P/BioT70 DNA in the presence of SSB and this solution is rapidly mixed in a stopped-flow instrument with a solution containing Cy3P/BioT70 DNA pre-bound by SSB, and FRET is monitored. Under these conditions, all Cy5-PCNA is pre-loaded onto the unlabeled P/BioT70 DNA substrate and stabilized by SSB prior to mixing, and the only pathway for dissociation of Cy5-PCNA into solution is through spontaneous opening of PCNA. Hence, RFC-catalyzed loading of Cy5-PCNA onto Cy3P/BioT70 DNA is rate-limited by spontaneous opening of PCNA. The loading trace was fit to a single-exponential and the rate constant is reported. Very similar values are obtained with RPA on the P/BioT33 P/T DNA substrates, indicating that the stability of PCNA encircling a P/T junction is the same when the adjacent ssDNA is bound by either RPA or SSB. *C*, monoubiquitination of loaded PCNA in the presence of a ssDNA-binding protein. *Top*, schematic representation of the experiment. PCNA was pre-assembled onto a P/BioT P/T DNA substrate in the presence of a stoichiometric amount of a ssDNA-binding protein and then monoubiquitination of target proteins was monitored as described in Figs. 1 and 2. *Bottom*, extent of PCNA monoubiquitination. The percentage of PCNA monomers that are monoubiquitinated is plotted as a function time. Symbols are indicated in the figure legends and the data for each represent the average ± S.D. of three independent experiments.

fuses off the ssDNA end upon release from RFC (Fig. 4*A*, *Condition 3*) (35) and excess Rad6/Rad18 does not compensate (Fig. 4*A*, *Condition 6*). Under these conditions, 63% of PCNA monomers are monoubiquitinated at 8 h incubation (Fig. 4*C*, *Condition 4*), similar to that observed when either NeutrAvidin or biotin are omitted. Altogether, this confirms that RPA significantly enhances Rad6/Rad18-catalyzed monoubiquitination of PCNA encircling a P/T junction by prohibiting diffusion of PCNA along the adjacent ssDNA. The results from Fig. 3 confirm that RPA directly interacts with Rad6/Rad18 and this direct interaction is significantly enhanced upon binding of RPA to ssDNA (8, 10). Thus, direct interactions between Rad6/Rad18 and RPA on ssDNA may also affect monoubiquitination of PCNA encircling P/T junctions, as previously suggested (8, 10). To directly test this, we utilized the *Escherichia coli* ssDNA-binding protein, SSB.

SSB is a functional homolog of human RPA and binds ssDNA noncooperatively and with very tight affinity (in pM range) at 200 mM ionic strength (28, 29, 37–39). We previously demonstrated that, like RPA, SSB binds tightly to ssDNA adjacent to a P/T junction and restricts PCNA to the upstream duplex region by physically blocking diffusion of the sliding clamp along the adjacent ssDNA (36). SSB is a homotetramer that binds ssDNA with an occluded site size of 65 nt at 200 mM ionic strength where the ssDNA is fully wrapped around SSB, contacting each subunit within the homotetramer. This differential mode of ssDNA-binding has no effect on the amount of PCNA loaded onto and maintained at P/T junctions (36), the orientation of PCNA encircling P/T junctions (Fig. 5*A*) (36), or the intrinsic stability of PCNA encircling P/T junctions (Fig. 5*B*). However, unlike RPA, SSB does not interact with Rad6/Rad18 (8, 10). These unique behaviors were exploited to decipher any effects of ssDNA·RPA·Rad6/Rad18 interactions (Fig. 3*E*) on monoubiquitination of PCNA encircling a P/T junction (Fig. 4*B*).

First, PCNA was pre-assembled on a P/T DNA substrate in the presence of a stoichiometric amount of a ssDNA-binding protein; SSB for P/BioT70 and RPA for P/BioT33 (Fig. 5*C*, *top*). Monoubiquitination of PCNA was then monitored over time as described above. Under these conditions, a single ssDNA-binding protein is adjacent to a P/T junction that is encircled by PCNA. On each DNA substrate, the same amount of PCNA is loaded onto the P/T junction and stabilized in the same orien-

tation (Fig. 5, *A* and *B*) (35, 36). Furthermore, RPA/ssDNA complexes do not directly activate Rad6/Rad18 catalysis (Fig. 2). Hence, any observed differences in PCNA monoubiquitination are because of interactions between Rad6/Rad18 and the RPA/ssDNA complex adjacent to the P/T junction. As observed in Fig. 5*C*, monoubiquitination of loaded PCNA is independent of the identity of the ssDNA-binding protein and this behavior is observed at two Rad6/Rad18 concentrations. Altogether, these results indicate that direct interactions, if any, between Rad6/Rad18 and the RPA/ssDNA complex adjacent to a P/T junction do not affect monoubiquitination of the resident PCNA. Hence, the enhancement of PCNA monoubiquitination on P/T DNA observed in the presence of RPA (Fig. 4) is because of a single RPA stabilizing PCNA at the P/T junction by physically blocking diffusion of the sliding clamp along the adjacent ssDNA.

Discussion

RPA is the most abundant ssDNA-binding protein in human cells and this high concentration is maintained throughout the cell cycle (26, 27). Furthermore, human RPA binds to ssDNA with extremely high affinity ($K_D \sim$ fM to pM) at physiological ionic strength (28, 29). Together, this ensures that RPA immediately coats exposed ssDNA, protecting it from degradation and preventing formation of alternative DNA structures (4). RPA also directly engages in DNA metabolism through protein·protein interactions. For example, under native conditions when ssDNA exposure is minimal, free RPA binds the p53 tumor suppressor protein in the nucleoplasm and inhibits binding of p53 to transcriptional promoters. Upon generation of persistent ssDNA regions, RPA binds tightly to the exposed templates, releasing and activating p53 (40–42). Furthermore, RPA bound to exposed ssDNA directly recruits various proteins involved in DNA repair pathways and the DNA damage checkpoint/response (43). Our studies on human Rad6/Rad18 now reveal that RPA can regulate the activity of a protein complex both in the nucleoplasm and on exposed ssDNA.

ssDNA mediates RPA·Rad18 interactions

The results from Fig. 3 indicate that 1) RPA and Rad18 interact in solution, albeit weakly, in agreement with previous *in vivo* and *in vitro* studies (8); 2) ssDNA-bound RPA directly interacts with Rad6/Rad18 at physiological ionic strength; and 3) ssDNA enhances the affinity of RPA for Rad6/Rad18. Altogether, these results confirm previous hypotheses (8, 10). When bound to ssDNA, OB folds A and B of RPA70, the primary ssDNA-binding sites of RPA, are occupied by ssDNA (28–30) and, hence, unlikely to bind Rad18. Previous independent reports revealed that transactivator proteins directly compete with ssDNA for binding to the ssDNA-binding OB folds of RPA70 (44, 45). Particularly, binding of ssDNA and p53 to RPA are mutually exclusive and such behavior is critical for p53 regulation in human cells (40–42, 46). These transactivator proteins directly bind RPA through "acidic patches" that may adopt negatively charged, amphipathic helices that structurally mimic ssDNA binding to an OB fold of RPA (45, 47–49). The portion of Rad18 that interacts with RPA contains many acidic residues (Fig. S1). Specifically, amino acid sequence 171–189 is ~30% D/E and may serve as an "acidic patch" to interact directly with RPA70. Given the overlap in RPA70-binding sites for p53 and Rad18, the results in Fig. 3 suggest that binding of ssDNA and Rad18 to RPA70 are also mutually exclusive. Hence, the interaction between RPA and Rad18 on ssDNA is entirely governed by the second Rad18-binding site within the RPA32 subunit.

OB-D of RPA32 is tightly engaged with extended ssDNA regions at physiological ionic strength whereas the WH domain plays no role in ssDNA binding and remains available for protein interactions (27). Also, binding of ssDNA by the RPA complex induces pronounced conformational rearrangements that further expose the RPA32 subunit, making it a better substrate for protein interaction (33, 34). Thus, we propose that Rad18 binds the WH domain of RPA32. Accordingly, Rad18 must contain independent binding sites for RPA70 and RPA32 as the binding interfaces of the RPA70 OB folds and the RPA32 WH domain are distinct (49, 50).

RPA inhibits monoubiquitination of PCNA in solution

For PCNA monoubiquitination to occur, Rad6/Rad18 must be in an active conformation and interact productively with PCNA. Regarding the former, Rad18 must remain a homodimer and Rad6 must bind the Rad18 homodimer at two independent binding sites (4, 5, 7, 51, 52). Rad18 monoubiquitination, which requires homodimerization of Rad18 (25), is robust in the absence of RPA and ssDNA (Fig. 1). Furthermore, Rad6 monoubiquitination is negligible and polyubiquitin chain formation is not observed. Finally, monoubiquitination of free PCNA is quite significant over a biologically relevant time course, with ubiquitin attached 70.74 ± 6.756% of all PCNA homotrimers on average. Altogether, this indicates that functional interactions between the Rad18 homodimer and Rad6 are achieved and maintained in the absence of RPA and ssDNA, and functional Rad6/Rad18 interacts productively with free PCNA in solution.

Monoubiquitinated PCNA is only observed on chromatin after exposure of human cells to agents that generate persistent stretches of RPA-coated ssDNA (4, 6, 7, 17, 18). This stringent selectivity is critical as aberrant PCNA monoubiquitination leads to increases in both spontaneous and damaged-induced mutagenesis (53). Interestingly, ubiquitin-specific protease 1 (USP1), the primary deubiquitinase for PCNA, is dramatically down-regulated throughout G_1 when more than 80% of the PCNA pool resides in the nucleoplasm (13–16, 19–23). A similar scenario arises in S-phase when USP1 is degraded or inactivated in response to genotoxic agents that cause fork uncoupling (2, 54). The results presented in Figs. 3 and 4 indicate that ssDNA-free RPA directly interacts with Rad6/Rad18 and inhibits monoubiquitination of free PCNA. Such behavior may compensate for loss of USP1 by preventing monoubiquitination of free PCNA and, hence, maintain the selectivity of PCNA monoubiquitination in the absence of USP1.

Inhibition of free PCNA monoubiquitination by RPA is directly and completely reversed by binding of ssDNA to RPA (Fig. 3). Under all conditions tested, monoubiquitination of Rad18 is not significantly affected (Fig. 2), mixed ubiquitin chain formation (Fig. S9) is not observed, and the occupancy of Rad6 within Rad6/Rad18 is maintained (Fig. 3). Collectively,

this indicates that RPA does not alter the composition of Rad6/Rad18; the Rad18 homodimer remains intact and maintains contact (via R6B) with the noncovalent ubiquitin-binding site on Rad6. RPA may regulate Rad6/Rad18 activity by mediating the Rad18 RING·Rad6 interaction in a ssDNA-dependent manner. In a previous report, full-length human Rad18 containing the RING domain inhibited polyubiquitin chain formation by Rad6 as well as Rad6 monoubiquitination. However, the isolated R6B was only sufficient to inhibit polyubiquitin chain formation and had no effect on Rad6 monoubiquitination, suggesting the Rad18 RING·Rad6 interaction may inhibit Rad6 monoubiquitination and promote PCNA monoubiquitination (7). If RPA mediates the Rad18 RING·Rad6 interaction, the effects of RPA on monoubiquitination of Rad6 and PCNA should be inversely correlated. Such behavior is clearly evident in the presence and absence of ssDNA (Fig. 2), in agreement with the proposed model. However, alternative models are also possible. For example, Rad6/Rad18 must productively bind PCNA for monoubiquitination to occur (7). Hence, RPA may regulate the activity of Rad6/Rad18 by mediating the Rad18·PCNA interaction in a ssDNA-dependent manner. Future studies will decipher these and other models.

RPA enhances monoubiquitination of PCNA encircling stalled P/T junctions

RPA promotes monoubiquitination of PCNA at persistent ssDNA regions generated throughout the cell cycle and such regulation is required for this PTM (8, 9, 13, 16). The results presented in Fig. 4 reveal that this is achieved, at least partially, by RPA stabilizing PCNA at P/T junctions by physically blocking diffusion of PCNA along the adjacent ssDNA. The results presented in Fig. 3 confirm that RPA directly interacts with Rad6/Rad18 and this interaction is significantly enhanced by binding of RPA to ssDNA. Thus, ssDNA/RPA complexes can directly recruit Rad6/Rad18 to the vicinity of stalled P/T junctions, as previously proposed (8, 10).

The extent and lifetime of such recruitment and whether it affects monoubiquitination of PCNA on DNA depends on the relative binding affinities of Rad6/Rad18 for an RPA/ssDNA complex and PCNA encircling stalled P/T junctions. To test this, we directly compared monoubiquitination of PCNA encircling a P/T junction abutted by either a single RPA or a single SSB (Fig. 5); only the former interacts with Rad6/Rad18 (8, 10). Under these conditions, any observed differences in PCNA monoubiquitination are attributed to interactions between Rad6/Rad18 and the RPA adjacent to the P/T junction. As the reaction progresses, the fraction of PCNA that is monoubiquitinated (*i.e.* reaction product) increases. This mimics S-phase in human cells after UV treatment where monoubiquitinated PCNA builds up and persists on ssDNA regions for many hours post UV (9, 55, 56). A relatively high affinity of Rad6/Rad18 for the RPA/ssDNA complex would inhibit PCNA monoubiquitination over time compared with SSB as the accumulating reaction products immobilize Rad6/Rad18, impeding turnover. In contrast, a relatively weak affinity favors direct binding of PCNA by Rad6/Rad18 from solution and localizes Rad6/Rad18 to an RPA/ssDNA complex only transiently, if at all, permitting efficient turnover throughout the incubation even as products accumulate. The results presented in Fig. 5 indicate that PCNA monoubiquitination is independent of the identity of the ssDNA-binding protein. Thus, the affinity of Rad6/Rad18 for the RPA/ssDNA complex is relatively weak compared with PCNA, and direct interactions, if any, between Rad6/Rad18 and the RPA/ssDNA complex do not affect monoubiquitination of the resident PCNA. However, these results do not rule out that weak, transient interactions selectively enhance monoubiquitination of PCNA on longer RPA-coated ssDNA regions. In human cells, persistent ssDNA regions generated at UV-induced lesions are 150–1250 nt in length, with the latter representing ~65% (2). Here, the effective concentration of RPA near stalled P/T junctions is much higher (~5- to 42-fold) than the resident PCNA and, hence, would promote interactions of Rad6/Rad18 with RPA along the ssDNA (28–30). These interactions may foster "successful collisions" between Rad6/Rad18 and the resident PCNA without significantly increasing the lifetime of Rad6/Rad18 on RPA-coated ssDNA. This unique model is the focus of future of studies. Altogether, the results presented in Figs. 3–5 suggest that after DNA replication stress, RPA binds the ssDNA exposed downstream of stalled P/T junctions and restricts the resident PCNAs to the upstream duplex regions by physically blocking diffusion of PCNA along ssDNA. This activity is required for efficient monoubiquitination of PCNA on DNA. Furthermore, Rad6/Rad18 directly interacts with RPA/ssDNA complexes, albeit weakly, and these interactions may promote monoubiquitination of PCNA on lengthy RPA-coated ssDNA regions.

RPA is critical for PCNA monoubiquitination as knockdown to undetectable levels in human and budding yeast cells effectively eliminates this PTM on DNA after treatment with replication-blocking agents (8, 9). Additional cellular factors have also been implicated to various extents (4) and new discoveries continue to emerge (57, 58). Some have been shown to bind Rad18 and/or PCNA and may promote PCNA monoubiquitination through direct interactions with these proteins. Future biochemical and cellular studies are needed to elucidate the mechanism(s) by which each factor promotes PCNA monoubiquitination and to decipher how these distinct pathways for regulation are interconnected *in vivo*.

Experimental procedures

Recombinant human proteins

Detailed information about plasmid construction and the expression, purification, and labeling of proteins can be found in the supporting information.

Oligonucleotides

Oligonucleotides were synthesized by Integrated DNA Technologies (Coralville, IA), purified on denaturing polyacrylamide gels, and the concentrations were determined from the absorbance at 260 nm using the calculated extinction coefficients. For annealing the DNA substrates (Fig. S6), the primer and corresponding complementary template strands were mixed in equimolar amounts in 1× Annealing Buffer (10 mM Tris-HCl, pH 8.0, 100 mM NaCl, 1 mM EDTA), heated to 95 °C for 5 min, and slowly cooled to room temperature.

Antibodies

Primary antibodies for PCNA (PC5, mouse monoclonal IgG1), RPA70 (MA70-2, mouse monoclonal IgG1), RPA32 (MA34, mouse monoclonal IgG1), RPA14 (mouse monoclonal IgG1), and Rad18 (H-77, rabbit polyclonal IgG), and secondary antibodies (goat anti-rabbit IgG-HRP) were purchased from Santa Cruz Biotechnology. Rad6 primary antibody (rabbit polyclonal IgG) was purchased from Abcam.

Ubiquitination assays

All ubiquitination assays were performed at room temperature (23 ± 2 °C) in 1× ubiquitination assay buffer (25 mM HEPES, pH 7.5, 10 mM $Mg(OAc)_2$, 125 mM KOAc) supplemented with 0.1 mg/ml BSA and 1 mM TCEP, and the final ionic strength was adjusted to physiological (200 mM) by the addition of appropriate amounts of KOAc. Detailed information can be found in the supporting information.

Analytical gel filtration

Experiments were performed at 4 °C on an ÄKTA purifier (GE Healthcare) using a Superdex 200 10/300 GL column (GE Healthcare) in 1× ubiquitination assay buffer supplemented with 1 mM TCEP, and the final ionic strength was adjusted to physiological (200 mM) by the addition of appropriate amounts of KOAc. Rad6/Rad18, RPA, and poly$(dT)_{33}$, or pre-incubated complexes thereof, were loaded in a volume of 150 μl. Concentrations of each are indicated in the respective figure/figure legend. The elution profile was analyzed by UV absorbance. Where indicated, fractions of a given elution profile were collected, resolved on 4–20% Mini-PROTEAN® TGX™ Gels, and visualized by Coomassie Blue staining or Western blotting with Rad6 antibody. Western blots were quantified and normalized to a Rad6 loading control.

Fluorescence microscopy

All experiments were performed at room temperature (23 ± 2 °C) in 1× ubiquitination assay buffer supplemented with 0.1 mg/ml BSA and 1 mM TCEP, and the final ionic strength was adjusted to physiological (200 mM) by the addition of appropriate amounts of KOAc. For steady-state fluorescence, measurements were done in Jobin Yvon FluoroMax-4 Fluorimeter. Assay solutions contained 110 nM Cy3-labeled P/T DNA (either Cy3P/BioT33 or Cy3P/BioT70), NeutrAvidin (0 or 440 nM), 1 mM ATP, and either an ssDNA-binding protein (0 or 110 nM of RPA or SSB) or Rad6·$(Rad18)_2$ (0 or 600 nM). To these solutions, Cy5-PCNA (100 nM homotrimer) and RFC (0 or 100 nM) were sequentially added. FRET was then measured at equilibrium as described previously (35, 36). For pre–steady-state fluorescence, studies were performed on an Applied Photophysics SX20 Stopped-Flow machine equipped with a fluorescence detector. In syringe A, Cy5-PCNA (180 nM homotrimer) was loaded by RFC (180 nM with 1 mM ATP) onto an unlabeled P/BioT DNA substrate (200 nM either P/BioT33 or P/BioT70 with 800 nM NeutrAvidin) that was pre-incubated with an ssDNA-binding protein (400 nM of either RPA or SSB). This solution was then rapidly mixed in a stopped-flow instrument with an equal volume from syringe B containing ATP (1 mM) and a Cy3P/BioT DNA substrate (200 nM either Cy3P/BioT33 or Cy3P/BioT70 with 800 nM NeutrAvidin) that was pre-incubated with an ssDNA-binding protein (400 nM of either RPA or SSB) and FRET was monitored over time as described previously (35). Loading traces were fit to a single-exponential increase and normalized to their respective ranges.

Author contributions—M. H. conceptualization; M. H., M. A., and A. P. data curation; M. H. formal analysis; M. H. supervision; M. H., M. A., and A. P. investigation; M. H., M. A., and A. P. methodology; M. H. writing-original draft; M. H. and S. J. B. project administration; M. H. and S. J. B. writing-review and editing; S. J. B. resources; S. J. B. software; S. J. B. funding acquisition.

Acknowledgment—We thank Dr. Titia K. Sixma who generously provided the plasmids for expression of Rad6/Rad18.

References

1. Hedglin, M., Kumar, R., and Benkovic, S. J. (2013) Replication clamps and clamp loaders. *Cold Spring Harb. Perspect. Biol.* **5,** a010165 CrossRef Medline
2. Hedglin, M., and Benkovic, S. J. (2017) Eukaryotic translesion DNA synthesis on the leading and lagging strands: Unique detours around the same obstacle. *Chem. Rev.* **117,** 7857–7877 CrossRef Medline
3. Yoon, J. H., Prakash, S., and Prakash, L. (2012) Requirement of Rad18 protein for replication through DNA lesions in mouse and human cells. *Proc. Natl. Acad. Sci. U.S.A.* **109,** 7799–7804 CrossRef Medline
4. Hedglin, M., and Benkovic, S. J. (2015) Regulation of Rad6/Rad18 activity during DNA damage tolerance. *Annu. Rev. Biophys.* **44,** 207–228 CrossRef Medline
5. Huang, A., Hibbert, R. G., de Jong, R. N., Das, D., Sixma, T. K., and Boelens, R. (2011) Symmetry and asymmetry of the RING-RING dimer of Rad18. *J. Mol. Biol.* **410,** 424–435 CrossRef Medline
6. Notenboom, V., Hibbert, R. G., van Rossum-Fikkert, S. E., Olsen, J. V., Mann, M., and Sixma, T. K. (2007) Functional characterization of Rad18 domains for Rad6, ubiquitin, DNA binding and PCNA modification. *Nucleic Acids Res.* **35,** 5819–5830 CrossRef Medline
7. Hibbert, R. G., Huang, A., Boelens, R., and Sixma, T. K. (2011) E3 ligase Rad18 promotes monoubiquitination rather than ubiquitin chain formation by E2 enzyme Rad6. *Proc. Natl. Acad. Sci. U.S.A.* **108,** 5590–5595 CrossRef Medline
8. Davies, A. A., Huttner, D., Daigaku, Y., Chen, S., and Ulrich, H. D. (2008) Activation of ubiquitin-dependent DNA damage bypass is mediated by replication protein A. *Mol. Cell* **29,** 625–636 CrossRef Medline
9. Niimi, A., Brown, S., Sabbioneda, S., Kannouche, P. L., Scott, A., Yasui, A., Green, C. M., and Lehmann, A. R. (2008) Regulation of proliferating cell nuclear antigen ubiquitination in mammalian cells. *Proc. Natl. Acad. Sci. U.S.A.* **105,** 16125–16130 CrossRef Medline
10. Huttner, D., and Ulrich, H. D. (2008) Cooperation of replication protein A with the ubiquitin ligase Rad18 in DNA damage bypass. *Cell Cycle* **7,** 3629–3633 CrossRef Medline
11. Game, J. C., and Chernikova, S. B. (2009) The role of RAD6 in recombinational repair, checkpoints and meiosis via histone modification. *DNA Repair* **8,** 470–482 CrossRef Medline
12. Masuyama, S., Tateishi, S., Yomogida, K., Nishimune, Y., Suzuki, K., Sakuraba, Y., Inoue, H., Ogawa, M., and Yamaizumi, M. (2005) Regulated expression and dynamic changes in subnuclear localization of mammalian Rad18 under normal and genotoxic conditions. *Genes Cells* **10,** 753–762 CrossRef Medline
13. Cotto-Rios, X. M., Jones, M. J., Busino, L., Pagano, M., and Huang, T. T. (2011) APC/CCdh1-dependent proteolysis of USP1 regulates the response to UV-mediated DNA damage. *J. Cell Biol.* **194,** 177–186 CrossRef Medline

14. Ogi, T., Limsirichaikul, S., Overmeer, R. M., Volker, M., Takenaka, K., Cloney, R., Nakazawa, Y., Niimi, A., Miki, Y., Jaspers, N. G., Mullenders, L. H., Yamashita, S., Fousteri, M. I., and Lehmann, A. R. (2010) Three DNA polymerases, recruited by different mechanisms, carry out NER repair synthesis in human cells. *Mol. Cell* **37,** 714–727 CrossRef Medline
15. Soria, G., Podhajcer, O., Prives, C., and Gottifredi, V. (2006) P21Cip1/WAF1 down-regulation is required for efficient PCNA ubiquitination after UV irradiation. *Oncogene* **25,** 2829–2838 CrossRef Medline
16. Yang, Y., Durando, M., Smith-Roe, S. L., Sproul, C., Greenwalt, A. M., Kaufmann, W., Oh, S., Hendrickson, E. A., and Vaziri, C. (2013) Cell cycle stage-specific roles of Rad18 in tolerance and repair of oxidative DNA damage. *Nucleic Acids Res.* **41,** 2296–2312 CrossRef Medline
17. Tsuji, Y., Watanabe, K., Araki, K., Shinohara, M., Yamagata, Y., Tsurimoto, T., Hanaoka, F., Yamamura, K., Yamaizumi, M., and Tateishi, S. (2008) Recognition of forked and single-stranded DNA structures by human RAD18 complexed with RAD6B protein triggers its recruitment to stalled replication forks. *Genes Cells* **13,** 343–354 CrossRef Medline
18. Masuda, Y., Suzuki, M., Kawai, H., Suzuki, F., and Kamiya, K. (2012) Asymmetric nature of two subunits of RAD18, a RING-type ubiquitin ligase E3, in the human RAD6A-RAD18 ternary complex. *Nucleic Acids Res.* **40,** 1065–1076 CrossRef Medline
19. Cooper, G. M., and Hausman, R. E. (2016) *The Cell: A Molecular Approach*, 7th Ed., Sinauer Associates, Inc., Publishers, Sunderland, MA.
20. Bravo, R., and Macdonald-Bravo, H. (1987) Existence of two populations of cyclin/proliferating cell nuclear antigen during the cell cycle: Association with DNA replication sites. *J. Cell Biol.* **105,** 1549–1554 CrossRef Medline
21. Zessin, P. J., Sporbert, A., and Heilemann, M. (2016) PCNA appears in two populations of slow and fast diffusion with a constant ratio throughout S-phase in replicating mammalian cells. *Sci. Rep.* **6,** 18779 CrossRef Medline
22. Morris, G. F., and Mathews, M. B. (1989) Regulation of proliferating cell nuclear antigen during the cell cycle. *J. Biol. Chem.* **264,** 13856–13864 Medline
23. Sasaki, K., Kurose, A., and Ishida, Y. (1993) Flow cytometric analysis of the expression of PCNA during the cell cycle in HeLa cells and effects of the inhibition of DNA synthesis on it. *Cytometry* **14,** 876–882 CrossRef Medline
24. Hicke, L., Schubert, H. L., and Hill, C. P. (2005) Ubiquitin-binding domains. *Nat. Rev. Mol. Cell Biol.* **6,** 610–621 CrossRef Medline
25. Miyase, S., Tateishi, S., Watanabe, K., Tomita, K., Suzuki, K., Inoue, H., and Yamaizumi, M. (2005) Differential regulation of Rad18 through Rad6-dependent mono- and polyubiquitination. *J. Biol. Chem.* **280,** 515–524 CrossRef Medline
26. Beck, M., Schmidt, A., Malmstroem, J., Claassen, M., Ori, A., Szymborska, A., Herzog, F., Rinner, O., Ellenberg, J., and Aebersold, R. (2011) The quantitative proteome of a human cell line. *Mol. Syst. Biol.* **7,** 549 CrossRef Medline
27. Prakash, A., and Borgstahl, G. E. (2012) The structure and function of replication protein A in DNA replication. *Subcell. Biochem.* **62,** 171–196 CrossRef Medline
28. Kim, C., Snyder, R. O., and Wold, M. S. (1992) Binding properties of replication protein A from human and yeast cells. *Mol. Cell. Biol.* **12,** 3050–3059 CrossRef Medline
29. Kim, C., Paulus, B. F., and Wold, M. S. (1994) Interactions of human replication protein A with oligonucleotides. *Biochemistry* **33,** 14197–14206 CrossRef Medline
30. Nguyen, B., Sokoloski, J., Galletto, R., Elson, E. L., Wold, M. S., and Lohman, T. M. (2014) Diffusion of human replication protein A along single-stranded DNA. *J. Mol. Biol.* **426,** 3246–3261 CrossRef Medline
31. Elia, A. E., Wang, D. C., Willis, N. A., Boardman, A. P., Hajdu, I., Adeyemi, R. O., Lowry, E., Gygi, S. P., Scully, R., and Elledge, S. J. (2015) RFWD3-dependent ubiquitination of RPA regulates repair at stalled replication forks. *Mol. Cell* **60,** 280–293 CrossRef Medline
32. Flynn, R. L., and Zou, L. (2010) Oligonucleotide/oligosaccharide-binding fold proteins: A growing family of genome guardians. *Crit. Rev. Biochem. Mol. Biol.* **45,** 266–275 CrossRef Medline
33. Binz, S. K., Sheehan, A. M., and Wold, M. S. (2004) Replication protein A phosphorylation and the cellular response to DNA damage. *DNA Repair* **3,** 1015–1024 CrossRef Medline
34. Wold, M. S. (1997) Replication protein A: A heterotrimeric, single-stranded DNA-binding protein required for eukaryotic DNA metabolism. *Annu. Rev. Biochem.* **66,** 61–92 CrossRef Medline
35. Hedglin, M., and Benkovic, S. J. (2017) Replication protein A prohibits diffusion of the PCNA sliding clamp along single-stranded DNA. *Biochemistry* **56,** 1824–1835 CrossRef Medline
36. Hedglin, M., Aitha, M., and Benkovic, S. J. (2017) Monitoring the retention of human proliferating cell nuclear antigen at primer/template junctions by proteins that bind single-stranded DNA. *Biochemistry* **56,** 3415–3421 CrossRef Medline
37. Waldman, V. M., Weiland, E., Kozlov, A. G., and Lohman, T. M. (2016) Is a fully wrapped SSB-DNA complex essential for *Escherichia coli* survival? *Nucleic Acids Res.* **44,** 4317–4329 CrossRef Medline
38. Kim, C., and Wold, M. S. (1995) Recombinant human replication protein A binds to polynucleotides with low cooperativity. *Biochemistry* **34,** 2058–2064 CrossRef Medline
39. Sibenaller, Z. A., Sorensen, B. R., and Wold, M. S. (1998) The 32- and 14-kilodalton subunits of replication protein A are responsible for species-specific interactions with single-stranded DNA. *Biochemistry* **37,** 12496–12506 CrossRef Medline
40. Abramova, N. A., Russell, J., Botchan, M., and Li, R. (1997) Interaction between replication protein A and p53 is disrupted after UV damage in a DNA repair-dependent manner. *Proc. Natl. Acad. Sci. U.S.A.* **94,** 7186–7191 CrossRef Medline
41. Miller, S. D., Moses, K., Jayaraman, L., and Prives, C. (1997) Complex formation between p53 and replication protein A inhibits the sequence-specific DNA binding of p53 and is regulated by single-stranded DNA. *Mol. Cell. Biol.* **17,** 2194–2201 CrossRef Medline
42. Lin, Y. L., Chen, C., Keshav, K. F., Winchester, E., and Dutta, A. (1996) Dissection of functional domains of the human DNA replication protein complex replication protein A. *J. Biol. Chem.* **271,** 17190–17198 CrossRef Medline
43. Maréchal, A., and Zou, L. (2015) RPA-coated single-stranded DNA as a platform for post-translational modifications in the DNA damage response. *Cell Res* **25,** 9–23 CrossRef Medline
44. Stauffer, M. E., and Chazin, W. J. (2004) Physical interaction between replication protein A and Rad51 promotes exchange on single-stranded DNA. *J. Biol. Chem.* **279,** 25638–25645 CrossRef Medline
45. He, Z., Brinton, B. T., Greenblatt, J., Hassell, J. A., and Ingles, C. J. (1993) The transactivator proteins VP16 and GAL4 bind replication factor A. *Cell* **73,** 1223–1232 CrossRef Medline
46. Dutta, A., Ruppert, J. M., Aster, J. C., and Winchester, E. (1993) Inhibition of DNA replication factor RPA by p53. *Nature* **365,** 79–82 CrossRef Medline
47. Li, R., and Botchan, M. R. (1993) The acidic transcriptional activation domains of VP16 and p53 bind the cellular replication protein A and stimulate in vitro BPV-1 DNA replication. *Cell* **73,** 1207–1221 CrossRef Medline
48. Bochkarev, A., Pfuetzner, R. A., Edwards, A. M., and Frappier, L. (1997) Structure of the single-stranded-DNA-binding domain of replication protein A bound to DNA. *Nature* **385,** 176–181 CrossRef Medline
49. Bochkareva, E., Kaustov, L., Ayed, A., Yi, G. S., Lu, Y., Pineda-Lucena, A., Liao, J. C., Okorokov, A. L., Milner, J., Arrowsmith, C. H., and Bochkarev, A. (2005) Single-stranded DNA mimicry in the p53 transactivation domain interaction with replication protein A. *Proc. Natl. Acad. Sci. U.S.A.* **102,** 15412–15417 CrossRef Medline
50. Mer, G., Bochkarev, A., Gupta, R., Bochkareva, E., Frappier, L., Ingles, C. J., Edwards, A. M., and Chazin, W. J. (2000) Structural basis for the recognition of DNA repair proteins UNG2, XPA, and RAD52 by replication factor RPA. *Cell* **103,** 449–456 CrossRef Medline
51. Tateishi, S., Sakuraba, Y., Masuyama, S., Inoue, H., and Yamaizumi, M. (2000) Dysfunction of human Rad18 results in defective postreplication

repair and hypersensitivity to multiple mutagens. *Proc. Natl. Acad. Sci. U.S.A.* **97,** 7927–7932 CrossRef Medline

52. Huang, J., Huen, M. S., Kim, H., Leung, C. C., Glover, J. N., Yu, X., and Chen, J. (2009) RAD18 transmits DNA damage signalling to elicit homologous recombination repair. *Nat. Cell Biol.* **11,** 592–603 CrossRef Medline
53. Huang, T. T., Nijman, S. M., Mirchandani, K. D., Galardy, P. J., Cohn, M. A., Haas, W., Gygi, S. P., Ploegh, H. L., Bernards, R., and D'Andrea, A. D. (2006) Regulation of monoubiquitinated PCNA by DUB autocleavage. *Nat. Cell Biol.* **8,** 339–347 CrossRef Medline
54. Yu, C., Gan, H., Han, J., Zhou, Z. X., Jia, S., Chabes, A., Farrugia, G., Ordog, T., and Zhang, Z. (2014) Strand-specific analysis shows protein binding at replication forks and PCNA unloading from lagging strands when forks stall. *Mol. Cell* **56,** 551–563 CrossRef Medline
55. Diamant, N., Hendel, A., Vered, I., Carell, T., Reissner, T., de Wind, N., Geacinov, N., and Livneh, Z. (2012) DNA damage bypass operates in the S and G2 phases of the cell cycle and exhibits differential mutagenicity. *Nucleic Acids Res.* **40,** 170–180 CrossRef Medline
56. Brown, S., Niimi, A., and Lehmann, A. R. (2009) Ubiquitination and deubiquitination of PCNA in response to stalling of the replication fork. *Cell Cycle* **8,** 689–692 CrossRef Medline
57. Li, F., Ball, L. G., Fan, L., Hanna, M., and Xiao, W. (2018) Sgs1 helicase is required for efficient PCNA monoubiquitination and translesion DNA synthesis in *Saccharomyces cerevisiae*. *Curr. Genet.* **64,** 459–468 CrossRef Medline
58. Wang, Z., Huang, M., Ma, X., Li, H., Tang, T., and Guo, C. (2016) REV1 promotes PCNA monoubiquitylation through interacting with ubiquitylated RAD18. *J. Cell Sci.* **129,** 1223–1233 CrossRef Medline